EPJ Web of Conferences **357**, 01001 (2026) https://doi.org/10.1051/epjconf/202635701001
ICAMC 2025

Development of $Cu_2NiSnSe_4$ Nanocrystals: Effects of Annealing on Structural and Electrical Properties

Devika Rajan Sajitha[1], *S.Purushothaman*[2] *Shyju* Thankaraj Salammal[1,3]* and *Shamima* Hussain[4]*

[1]Centre of Excellence for Energy Research, Sathyabama Institute of Science and Technology, Chennai, India.
[2]School of Engineering and Technology, Jaipur National University, Jagatpura, Jaipur- 302017, Rajasthan, India.
[3]Centre for Nanoscience and Nanotechnology, Sathyabama Institute of Science and Technology, Chennai, India.
[4]UGC-DAE-CSR Kalpakkam Node, Kokilamedu, Tamilnadu, India

Abstract. This work investigates structural, electrochemical, and electrical enhancement of $Cu_2NiSnSe_4$ (CNTSe) synthesized by high-energy ball milling followed by post-annealing at 450°C. X-ray diffraction confirmed the formation of a tetragonal kesterite structure in both as-synthesised and annealed CNTSe with the annealed samples exhibiting markedly improved crystallinity and grain uniformity. FESEM results indicate that annealing leads to more uniform elemental distribution and promotes the development of well-defined grains. Hall measurements and electrochemical demonstrated superior electrical properties, including a high Specific capacitance of 1380.93 F/g and Electrical conductivity of 6.08×10^3 (mho. cm) and a narrow band gap of 1.1 eV suitable for harvesting solar energy. These finding highlights the crucial role of annealing in optimizing CNTSe for solar cell and supercapacitor applications. Moreover, the mechanochemical synthesis route provides a simple, scalable, eco-friendly method of developing semiconducting materials for advanced energy technologies.

1 Introduction

Research on photovoltaic (PV) and energy storage technologies has increased due to the increasing demand for clean and renewable energy sources on a worldwide scale. Despite being the industry leader, The negative aspects of the traditional silicon based solar cells includes high production costs, energy-intensive manufacturing procedures, and limited adaptability. Because of their high absorption coefficients, configurable bandgaps, and material compatibility with scalable, economical production, thin-film chalcogenide semiconductors have become feasible alternatives[1]. Among these, semiconductor families like CdTe, $CuInSe_2$ (CIS), and $Cu(In,Ga)Se_2$ (CIGS) have achieved remarkable efficiencies above 22% [2]; nevertheless, their sustainable deployment is limited by their reliance on rare or environmentally dangerous materials. The development of non-toxic, earth-abundant semiconductors has become a key priority for next-generation photovoltaic absorbers. Kesterite-structured quaternary chalcogenides have drawn a lot of interest as potential substitutes, especially Cu_2ZnSnS_4 (CZTS) and $Cu_2ZnSnSe_4$ (CZTSe)[3]. They show excellent optoelectrical properties required for the efficient solar energy conversion, absorption coefficients on the order of 10^4 cm^{-1}, and ideal direct bandgaps between 1.0 and 1.5 eV. The technological promise of thin films based on CZTSSe have been shown by the achievement of device efficiencies of up to 14.9%[4]. Device performance, charge transfer, and open-circuit voltage are restricted by enduring problems such secondary phases, anti-site disorder, and the kesterite structure has narrow stability field. The tetrahedral structure is maintained while the electronic structure is tuned using substitutional engineering, specifically the substitution of Ni^{2+} for Zn^{2+}. In recent investigations, Ni-substituted kesterites such as Cu_2NiSnS_4 (CNTS) and $Cu_2NiSnSe_4$ (CNTSe) have demonstrated interesting optoelectronic characteristics[5–7]. Ni can be added to the absorber layer to improve its electrical conductivity and tune the optical bandgap to characteristics that are ideal for single-junction photovoltaics. Power conversion efficiency a maximum of 17.06% have been projected by theoretical device simulations for Ni-based systems, highlighting their latent potential in comparison to Zn-based kesterites[8].

Because of their high surface activity, narrow bandgaps, efficient charge transfer, quaternary chalcogenides are becoming more common in solar cells, batteries and supercapacitors for energy storage and conversion[9]. Significant capacitance has been shown by kesterite-based selenides and sulfides, indicating potential in hybrid systems that combine solar energy harvesting and charge storage. CNTSe is a promising contender for advanced energy applications because to its direct bandgap, high absorption coefficient, and structural flexibility. Recently, mechanosynthesis has become a popular and environmentally friendly method for directly synthesizing nanocrystalline quaternary chalcogenides from precursors[10]. This technique successfully

*Email: shyjuantony1983@gmail.com.

increases crystallinity, lowers lattice strain, suppresses secondary phases, and improves the overall optoelectronic performance of kesterite materials when paired with optimal annealing procedures[11].

This study reports the mechanochemical synthesis of CNTSe nanocrystals followed by systematic annealing to investigate their electrical, electrochemical, and structural properties. Heat treatment significantly enhances carrier mobility, energy storage, and crystallographic ordering, improving phase purity, crystallite size, and conductivity. These results position CNTSe as a promising material for supercapacitor electrodes and photovoltaic absorbers in sustainable energy applications.

2 Materials and Methods

Highly purified (≥ 99.9%) elemental powders of copper, nickel, tin and selenium were used to develop CNTSe. The components underwent solvent-free mechanochemical processing after being weighed in a 2:1:1:4 molar ratio. Using a high-energy ball mill running at 2750 rpm for 10 hours with intermittent temperature controls, this sustainable synthesis was conducted in a chrome steel vial with 6 g of precursors and 18 g of stainless-steel balls. The procedure was designed to facilitate the formation of a single-phase product, which was subsequently confirmed through post-synthesis characterization[12]. CZTSe was prepared for reference and comparative investigations using the same methodology, which confirmed direct, efficient phase production via mechanosynthesis in the absence of a solvent or post-synthesis processing and was in compliance with methods documented in the literature. Upon synthesis, Pellets were formed by compressing CNTSe powder using a stainless-steel die at a uniaxial pressure of 180 MPa, guaranteeing sturdy, dense samples appropriate for further examination. A second set of pellets was annealed at 450°C for two hours at a high vacuum (10^{-6} mbar), whereas the first set was left as-synthesised. This temperature was selected based on optimized phase formation, improved crystallinity, and suppression of secondary phases. The as-synthesized CNTSe was previously prepared and validated by comparison with the standard CZTSe, and this paper now focuses entirely on the annealing of CNTSe. This made it possible to compare the impacts of post-synthesis thermal treatment on the material's physical and microstructure in a systematic manner[13].

The active CNTSe material (as-synthesised or annealed), carbon black (Super P) as a conductive addition, and polyvinylidene fluoride (PVDF) as a binder were used in an 8:1:1 weight ratio to produce electrodes for electrochemical tests [14]. N-methyl pyrrolidone (NMP) was incorporated into the mixture to produce a uniform slurry that was then applied on nickel foam (NF) substrates that were 3 × 1 cm^2 and 0.5 mm thick with total active mass of 3 mg. Before its use, the foam was cleaned ultrasonically with ethanol, deionized water, and 1 M HCl. Before electrochemical testing, the coated electrodes were dried in a vacuum oven at 60˚C for 12 hours.

To evaluate the structural, compositional, and functional characteristics, an extensive characterisation was carried out. X-ray diffraction (XRD) was used to confirm the purity and crystalline phase (Bruker D8 Advance, Cu Kα). Raman spectroscopy (Renishaw; 532 nm laser) further confirmed vibrational lattice modes. With the assistance of EDAX and field emission scanning electron microscopy (FESEM) (Zeiss Gemini), surface morphology and microstructure were investigated. Thermo K-Alpha's X-ray photoelectron spectroscopy (XPS) was utilized to ascertain the chemical states and elemental composition. A Bio-Logic SP-300 was used for electrochemical testing in a three-electrode configuration using 3 M KOH as the electrolyte. Optical properties were investigated utilizing a UV-Vis-NIR spectrophotometer (JASCO), while the electrical characteristics were examined using Hall effect measurements (ECOPIA HMS-7000).

3 Results and Discussion

Mechanochemistry was employed to develop the CNTSe material over a 10-hour period in a high-energy planetary ball mill[15]. The as-synthesized CNTSe, previously validated against CZTSe standards, upon annealing produced a similar single-phase tetragonal kesterite structure consistent with reference patterns [mp-1225885], as confirmed by XRD analysis. As seen in **Figure 1(a)**, both the as-synthesised and annealed samples had diffraction peaks indexing to the distinctive planes of kesterite structures, such as (112), (200), and (204). No secondary phases were found, showing high phase purity. The (112) and (204) reflections in particular showed a decrease in full width half maximum (FWHM) and a sharpening and intensification of XRD peaks upon annealing at 450 °C under high vacuum. This suggests that the annealed samples have improved crystallinity, grain coalescence, and decreased microstrain[16]. The crystallite size, as determined by the Debye-Scherrer equation $\boldsymbol{D = K\beta cos\theta}$, increased to about 23 nm, while microstrain and dislocation density dramatically dropped, indicating a decrease in lattice defects, as indicated in **Table 1**. The as-synthesised CNTSe displayed distinctive vibrational modes, including a significant A_1 symmetric selenium stretch at 174 cm^{-1} and metal–selenide bonding modes at 226 and 248 cm^{-1}, which were confirmed by Raman spectroscopy[17]. In accordance with better lattice ordering and less disorder, Raman peaks sharpened and slightly moved after annealing, with new significant peaks emerging at approximately 176, 212, and 233 cm^{-1} (**Figure 1(b)**)[13,18,19].

According to morphological insights from FESEM. The initially observed particle clusters undergo grain

growth and partial surface melting, facilitated by enhanced atomic diffusion at elevated temperatures. As a result, individual grains coalesce and merge, leading to the formation of larger agglomerates with a more cloud-like morphology, as illustrated in **Figure 2(a)**. This grain coarsening and intergranular fusion contribute to improved grain connectivity and structural uniformity.

Table 1: Crystallographic parameters, and lattice constants of the as-synthesized and Annealed CNTSe.

CNTSe	2Theta (deg.)		(hkl)	FWHM (rad.)	Crystallite size (nm)	d-spacing (Å)		Dislocation density (lines/m^2) 10^{-3}	Strain 10^{-3}	Lattice parameters (a=b=c) (Å)			
										a		c	
	Exp	Cal				Exp	Cal			Exp	Cal	Exp	Cal
Assynthesized	**27.12**	**27.19**	**(112)**	**0.0158**	**12.101**	**3.284**	**3.277**	**2.14 ×10^{15}**	**1.291**	**5.690**	**5.689**	**11.40**	**11.39**
Annealed	**27.217**	**27.19**	**(112)**	**0.00611**	**23.3**	**3.276**	**3.277**	**1.84 ×10^{15}**	**8.117**	**5.665**	**5.693**	**11.34**	**11.33**

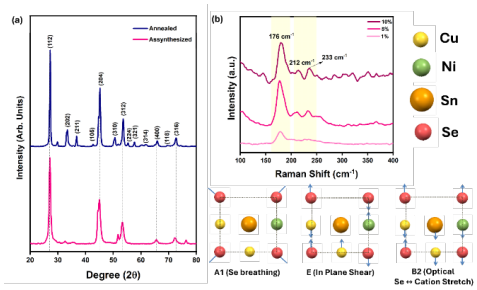

Figure 1: (a) X-ray diffraction patterns of as-synthesized and annealed CNTSe, highlighting the structural evolution upon annealing. (b) Raman spectra of annealed CNTSe recorded at different laser power percentages (1%, 5%, and 10%), the vibrational modes illustrated using the structural schematic inset.

Additionally, since the weight percentages 24.58, 14.56, 14.80, and 46.06 derived from the energy dispersive X-ray analysis (EDAX) spectrum closely resemble the initial composition ratio of 2:1:1:4 , indicating successful synthesis without appreciable element loss, verified that the elemental composition of CNTSe is consistent with the initial stoichiometric ratio (**Figure 2(b)**)[20].

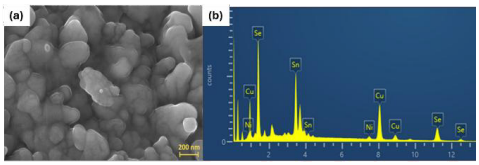

Figure 2: (a) FESEM image, (b) EDAX spectrum of annealed CNTSe**.**

The as-synthesised CNTSe exhibits an band gap of about 1.17 eV as shown in **Figure 3(a)** which makes it appropriate for near-infrared absorption in photovoltaic applications[21]. The band gap dropped to around 1.1 eV (**Figure 3(b)**) after annealing, increasing absorption in the near-infrared spectrum and perhaps enhancing optoelectronic performance which is calculated using Kubelka Munk function. The absorption coefficient (α), which is exactly proportional to the Kubelka-Munk function (F(R)), was determined by further processing the reflectance data from DRS using the Kubelka-Munk equation[22].

$$F(R) = \frac{K}{S} = \frac{(1-R)^2}{2R} \quad (1)$$

In **Figure 3(d)**, the additional optical characteristics are displayed with refractive index, extinction coefficient, optical conductivity, and dielectric constant saturating above 500 nm, the optical characteristics of annealed CNTSe exhibit significant wavelength dependent changes in the UV–visible region. An increased and stabilized refractive index, stronger optical conductivity, and an evident extinction coefficient in the visible range are examples of sharper and more consistent optical constants from the material's improved crystallinity and phase purity after annealing. Annealing CNTSe improves grain growth and reduces defects, enhancing light absorption and carrier mobility for more efficient photovoltaic performance.

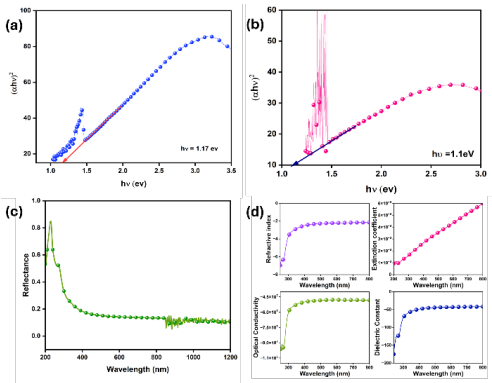

Figure 3: UV–Vis DRS analysis of CNTSe showing Kubelka–Munk plot for band gap of (a) as-synthesized, (b) annealed; Annealed CNTSe's (c) reflectance spectra, and (d) optical property variations (refractive index, extinction coefficient, dielectric constant, and optical conductivity).

Excellent energy storage characteristics are highlighted by the electrochemical characterisation, which showed a specific capacitance of 2155.87 F/g for the as-synthesised CNTSe at 3 mA/g current density. GCD curves (0.0–0.45 V) at 3–22 mA/g show longer

charge–discharge durations at lower currents, with all electrodes displaying linear profiles. Using the equation (2), the specific capacitance (C_s) has been calculated from discharge time.

$$C_s = \frac{I \times t_d}{m \times \Delta V} \quad (2)$$

Table 2: Hall Measurement data for As-synthesized and Annealed CNTSe.

CNTSe	Temperature (°C)	Carrier Concentration (cm^{-3})	Mobility ($cm^2V^{-1}s^{-1}$)	Resistivity (ohm. cm)	Conductivity (mho. cm)	Average Hall Co-efficient
As-synthesized	**RT**	**4.62×10^{19}**	**1.56**	**8.62×10^{-3}**	**1.15×10^{2}**	**0.135**
Annealed	**RT**	**3.75×10^{19}**	**1.01**	**1.65×10^{-4}**	**6.08×10^{3}**	**0.166**

Grain coalescence reduced the surface area of the annealed sample, which is why the annealed CNTSe showed a lower capacitance of 1380.93 F/g at 3 mA/g illustrated in Figure 4. However, impedance studies showed that the annealed sample had better charge transfer kinetics and lower resistance, indicating greater conductivity and electrochemical stability[23].

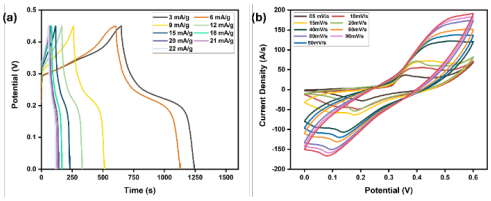

Figure 4: Electrochemical performance of CNTSe nanocrystals annealed at 450˚C.

According to Hall effect measurements, both samples showed p-type conductivity, where the bulk of the carriers are holes[24]. The electrical conductivity of the annealed CNTSe increased from 1.15×10^2 $(\Omega.cm)^{-1}$ (as-synthesized) to 6.08×10^3 $(\Omega.cm)^{-1}$, while the carrier concentration of annealed CNTSe is 3.75×10^{19} cm^3. According to the noted advancements in crystallography and decreased defect density, carrier mobility, Resistivity and Hall Co-efficient significantly differed as tabulated in **Table 2**. Because of improved crystallinity and fewer trapping sites, these electrical enhancements imply more effective charge transfer and decreased recombination. The results show that high-purity CNTSe with a distinct kesterite structure can be efficiently produced using the mechanochemical synthesis technique. Annealed CNTSe is a suitable compound for optical and electrical applications because of its substantial improvements in crystallinity, reduction of structural imperfections, electrical conductivity, and electrochemical performance upon subsequent annealing at 450 °C[12].

4 Conclusion

This study demonstrates that mechanochemical synthesis combined with optimized annealing at 450 °C provides a scalable and efficient route to high-purity CNTSe nanocrystals with tailored functional properties. Structural and spectroscopic analyses confirm that annealing enhances crystallinity, phase purity, grain uniformity, and elemental homogeneity, leading to a stable kesterite structure. These improvements result in a reduced band gap (~1.1 eV) and superior optical and electrical characteristics, enabling efficient light absorption and charge transport. The high specific capacitance (1380.93 F g^{-1}) further highlights the suitability of annealed CNTSe for electrochemical energy storage. Collectively, these attributes position CNTSe as a versatile, earth-abundant, and environmentally benign material with strong potential for use as an absorber layer in next-generation photovoltaic devices, electrode material for high-performance supercapacitors, and a multifunctional platform for integrated energy conversion and storage systems.

The authors express their gratitude to UGC-DAE-CSR, Govt of India, for the funding Project Ref. No. **CRS/2021-22/04/598**.

The data supporting the findings of this study are available upon reasonable request.

Devika Rajan Sajitha: Writing - original draft; Conceptualization; Methodology; Investigation; Data curation.
Shyju Thankaraj Salammal: Writing - review & editing; Supervision; Resources; Validation; Visualization.
Shamima Hussain: Writing - review & editing; Resources; Validation.

Reference

[1] E.T. Efaz1, M.M. Rhaman, S. Al Imam, K.L. Bashar, F. Kabir, M.E. Mourtaza, S.N. Sakib, F.A. Mozahid, A review of primary technologies of thin-film solar cells, Eng. Res. Express 3 (2021). https://doi.org/10.1088/2631-8695/ac2353.
[2] M. Powalla, S. Paetel, E. Ahlswede, R. Wuerz, C.D. Wessendorf, T. Magorian Friedlmeier, Thin-film solar cells exceeding 22% solar cell efficiency: An overview on CdTe-, Cu(In,Ga)Se 2 -, and perovskite-based materials, Appl. Phys. Rev. 5 (2018) 041602. https://doi.org/10.1063/1.5061809.
[3] T. Wada, S. Nakamura, T. Maeda, Ternary and multinary Cu-chalcogenide photovoltaic materials

from CuInSe 2 to Cu 2ZnSnS 4 and other compounds, Prog. Photovoltaics Res. Appl. 20 (2012) 520–525. https://doi.org/10.1002/pip.2183.

[4] Y. Li, C. Cui, H. Wei, Z. Shao, Z. Wu, S. Zhang, X. Wang, S. Pang, G. Cui, Suppressing Element Inhomogeneity Enables 14.9% Efficiency CZTSSe Solar Cells, Adv. Mater. (2024). https://doi.org/10.1002/adma.202400138.

[5] D. Shin, B. Saparov, D.B. Mitzi, Defect Engineering in Multinary Earth-Abundant Chalcogenide Photovoltaic Materials, Adv. Energy Mater. 7 (2017). https://doi.org/10.1002/aenm.201602366.

[6] A. Ghosh, D.K. Chaudhary, A. Biswas, R. Thangavel, G. Udayabhanu, Solution-processed Cu2XSnS4 (X = Fe, Co, Ni) photo-electrochemical and thin film solar cells on vertically grown ZnO nanorod arrays, RSC Adv. 6 (2016) 115204–115212. https://doi.org/10.1039/c6ra24149b.

[7] D.R. Sajitha, B. Stephen, A. Nakamura, M. Selvaraj, S.T. Salammal, S. Hussain, The emergence of chalcogenides: A new era for thin film solar absorbers, Prog. Solid State Chem. 76 (2024) 100490. https://doi.org/10.1016/j.progsolidstchem.2024.100490.

[8] M.R. Ali, T.M. Khan, Nurjahan-Ara, S.R. Al Ahmed, Numerical simulation to optimize the photovoltaic performances of Cu2ZnSnS4 solar cell with Cu2NiSnS4 as hole transport layer, J. Phys. Chem. Solids 197 (2025) 112448. https://doi.org/https://doi.org/10.1016/j.jpcs.2024.112448.

[9] G. Tseberlidis, C. Gobbo, V. Trifiletti, V. Di Palma, S. Binetti, Cd-free kesterite solar cells: State-of-the-art and perspectives, Sustain. Mater. Technol. 41 (2024) e01003. https://doi.org/https://doi.org/10.1016/j.susmat.2024.e01003.

[10] A. Wang, M. He, M.A. Green, K. Sun, X. Hao, A Critical Review on the Progress of Kesterite Solar Cells: Current Strategies and Insights, Adv. Energy Mater. 13 (2023). https://doi.org/10.1002/aenm.202203046.

[11] H. Wei, Y. Li, C. Cui, X. Wang, Z. Shao, S. Pang, G. Cui, Defect suppression for high-efficiency kesterite CZTSSe solar cells: Advances and prospects, Chem. Eng. J. 462 (2023) 142121. https://doi.org/https://doi.org/10.1016/j.cej.2023.142121.

[12] T.S. Shyju, S. Anandhi, R. Suriakarthick, R. Gopalakrishnan, P. Kuppusami, Mechanosynthesis, deposition and characterization of CZTS and CZTSe materials for solar cell applications, J. Solid State Chem. 227 (2015) 165–177. https://doi.org/10.1016/j.jssc.2015.03.033.

[13] J. Angel Agnes, D.R. Sajitha, S. Beauno, M. Selvaraj, S. Thankaraj Salammal, Efficient mechanochemical studies of Cu2FeSnSe4 quaternary chalcogenide for energy conversion and storage applications, Inorg. Chem. Commun. 173 (2025) 113881. https://doi.org/https://doi.org/10.1016/j.inoche.2024.113881.

[14] K. Narthana, G. Durai, P. Kuppusami, J. Theerthagiri, S. Sujatha, S.J. Lee, M.Y. Choi, One-step synthesis of hierarchical structured nickel copper sulfide nanorods with improved electrochemical supercapacitor properties, Int. J. Energy Res. 45 (2021) 9983–9998. https://doi.org/10.1002/er.6492.

[15] C. Suryanarayana, Mechanical alloying and milling, Prog. Mater. Sci. 46 (2001) 1–184. https://doi.org/10.1016/S0079-6425(99)00010-9.

[16] I. A., A.A. J., D. Rajan Sajitha, K.K. A.M., C. Govindasamy, K.M. Almutairi, B. S., S. Thankaraj Salammal, Exploration of structural and optoelectronic behaviour of mechanochemically synthesized earth-abundant phase pure Cu2FeSnSe4, Mater. Res. Bull. 189 (2025) 113477. https://doi.org/https://doi.org/10.1016/j.materresbull.2025.113477.

[17] D. Rajan, S. Thankaraj, V. Panneerselvam, Solvent free mechanosynthesis of Cu 2 NiSnSe 4 nanomaterials for high-performance energy devices, Mater. Sci. Eng. B 325 (2026) 119117. https://doi.org/10.1016/j.mseb.2025.119117.

[18] A. V. Stanchik, M.S. Tivanov, I.I. Tyukhov, R. Juskenas, O. V. Korolik, V.F. Gremenok, A.M. Saad, A. Naujokaitis, Temperature dependence of Raman scattering in the Cu2ZnSnSe4 thin films on a Ta foil substrate, Sol. Energy 201 (2020) 480–488. https://doi.org/10.1016/j.solener.2020.03.043.

[19] A.A. Johnrose, D. Rajan Sajitha, V. Panneerselvam, A. Sivaramalingam, K.K. Amirtharaj Mosas, B. Stephen, S. Thankaraj Salammal, Mechanochemically Synthesized Nanocrystalline Cu2ZnSnSe4 as a Multifunctional Material for Energy Conversion and Storage Applications, Nanomaterials 15 (2025). https://doi.org/10.3390/nano15241866.

[20] S. Jain, S. Kumar Swami, V. Dutta, S. Narain Sharma, Impact on Structural, Morphological, and compositional properties of CZTS thin films annealed in different environments, Inorg. Chem. Commun. 133 (2021) 108879. https://doi.org/https://doi.org/10.1016/j.inoche.2021.108879.

[21] X. Jiang, W. Xu, R. Tan, W. Song, J. Chen, Solvothermal synthesis of highly crystallized quaternary chalcogenide Cu 2 FeSnS 4 particles, Mater. Lett. (2013) 1–4. https://doi.org/10.1016/j.matlet.2013.03.102.

[22] T. Zhu, W.P. Huhn, G.C. Wessler, D. Shin, B. Saparov, D.B. Mitzi, V. Blum, I2-II-IV-VI4 (I = Cu, Ag; II = Sr, Ba; IV = Ge, Sn; VI = S, Se): Chalcogenides for Thin-Film Photovoltaics, Chem. Mater. 29 (2017) 7868–7879. https://doi.org/10.1021/acs.chemmater.7b02638.

[23] J. Paier, R. Asahi, A. Nagoya, G. Kresse, Cu2 ZnSnS4 as a potential photovoltaic material: A hybrid Hartree-Fock density functional theory study, Phys. Rev. B - Condens. Matter Mater. Phys. 79 (2009) 1–8. https://doi.org/10.1103/PhysRevB.79.115126.

[24] O. HEAVISIDE, Electrical Papers, 2019.